

## HEAVY FLAVORS\*

Brad Cox  
 Fermilab, Batavia, Illinois 60510

Frederick J. Gilman  
 Stanford Linear Accelerator Center, Stanford University  
 Stanford, California 94305

Thomas D. Gottschalk  
 California Institute of Technology  
 Pasadena, California 91125

Working Group Members: A. Abashian, Y. Arad, V. Barger, B. Barnett, D. Berley, C. Bromberg, C. Buchanan, J. Butler, L. Chau, J. Collins B. Cox, N. Deshpande, I. Dunitz, G. Feldman, F. Gilman, N. Glover, T. Gottschalk, G. Hanson, D. Hedin, S. Heppelmann, L. Jones, D. Judd, H. Kagan, J. Merlo, B. Milliken, M. Mishina, D. Morris, A. Odian, F. Paige, R. Panvini, L. Price, J. Ralston, D. Reeder, R. Ruchti J. Slaughter, D. Smith, A. Soni, D. Soper, T. Tauchi, G. Theodosiou, G. Trilling, D. Wagoner, S. Wojcicki

### Summary

We examine a range of issues pertaining to heavy flavors at the SSC, including heavy flavor production by gluon-gluon fusion and by shower evolution of gluon jets, flavor tagging, reconstruction of Higgs and W bosons, and the study of rare decays and CP violation in the  $B$  meson system. A specific detector for doing heavy flavor physics and tuned to this latter study at the SSC, the TASTER, is described.

### 1. Introduction

The topic of heavy flavors is central to doing much of the physics that is potentially capable of being explored at the SSC. Not only do long-sought particles like the Higgs boson decay preferentially into heavy quarks if  $M_H < 2 M_W$ , but the weak decays of hadrons containing heavy quarks, and especially their CP violating decays, are interesting in and of themselves because of the probe they provide of physics of the standard model and beyond. Moreover, the production mechanisms of heavy quarks are worthy of study in their own right, as they provide insight into structure functions, fragmentation, etc., and allow us to test QCD in both its perturbative and non-perturbative aspects.<sup>1</sup>

We begin our detailed report in Section 2 with the discussion of this last topic, heavy flavor production mechanisms and the corresponding rates, especially for the case of  $b$  quarks. The dominant production mechanism at low  $p_T$  is from gluon fusion, but for transverse momenta significantly larger than the quark mass of relevance, "flavor excitation" from the beam protons and QCD shower evolution from gluon jets become dominant.

We then turn to the key question of detecting the heavy quarks that are produced, i.e. flavor tagging. There is more optimism reflected in the present report than was found at the Snowmass Workshop of two years ago. A good part of it is based on recent results from using microvertex detectors in fixed target experiments to sort out successfully clean charm signals in the presence of very large backgrounds.<sup>2</sup> Variants of this technique, as well as other tagging schemes, are discussed in Section 3.

Section 4 goes on to the next step, that of using heavy quark flavors to look for new physics. The topics specifically addressed include detecting a Higgs boson decaying to bottom quarks, measuring continuum  $W$ -pair production with one  $W$  decaying leptonically and the other decaying to  $t$  and  $b$  quarks, and searching for a fourth generation heavy quark decaying to a  $W$  plus a  $t$  quark.

A different kind of heavy flavor physics involves looking at their weak decays. The production of heavy flavors at the SSC exceeds by many orders of magnitude the data sample available at any other accelerator envisioned until now. This could permit the study, for example, of rare decays of hadrons containing  $b$  quarks and the study of mixing and CP violation in the  $B$  meson system. Section 5 summarizes recent theoretical work on the subject of such rare decays, with emphasis on estimating branching ratios and CP violating asymmetries for experimentally accessible interesting modes. This is used as input, together with ideas of tagging using  $\psi \rightarrow \mu\mu$ , to Section 6. There, a preliminary design and some physics possibilities are presented for a detector, the TASTER. It is a semi-forward spectrometer for use at the SSC in carrying out rare decay and CP violation studies in the  $B$  meson system. The tentative outcome of the analysis of the capabilities of the TASTER, and in particular, the development of a trigger strategy for  $B$  mesons, encourages further exploration of the prospects for doing this kind of physics at the SSC.

### 2. Heavy Flavor Production Rates

For sufficiently heavy quarks, the dominant flavor production mechanism in QCD is gluon-gluon fusion:

$$g + g \rightarrow Q + \bar{Q}, \quad (1)$$

with total cross section

$$\sigma_{TOT}(Q\bar{Q}) \approx \int dx_1 dx_2 G(x_1, Q^2) G(x_2, Q^2) d\sigma[g + g \rightarrow Q + \bar{Q}]. \quad (2)$$

\* Work supported by the Department of Energy, contract DE-AC03-76SF00515.

In applying Eq. (2) a number of obvious questions come to mind:

1. What are the higher order corrections to Eq. (2) and are they numerically important?
2. How accurately is the gluon distribution function  $G(x, Q^2)$  in Eq. (2) known for the SSC kinematic region?
3. Is Eq. (1) the dominant production mechanism in all kinematic regimes?
4. How heavy is "sufficiently heavy"?

The validity of Eq. (2) has been examined in detail by Collins, Soper and Sterman.<sup>3</sup> They conclude that gluon fusion is indeed the dominant mechanism for the total flavor production cross sections, and that other mechanisms, such as "flavor excitation",

$$q + Q \rightarrow q + Q \text{ or } g + Q \rightarrow g + Q, \quad (3)$$

are relatively suppressed. Flavor production estimates are presently done using the lowest order  $2 \rightarrow 2$  QCD cross sections for Eq. (1). While full calculations of higher order perturbative QCD corrections have not yet been completed, the partial results in Ref. 4 suggest that these corrections should not be large. The largest source of uncertainty in Eq. (2) thus involves the parameterizations of the gluon distribution functions.

The reliability of heavy flavor production rates according to Eq. (2) has been investigated by McKay and Ralston.<sup>5</sup> For bottom production at SSC energies, Eq. (2) samples the gluon distribution function at extremely small  $x$  (e.g.,  $x < 10^{-6}$ ). For modest  $Q^2 \approx (2M_b)^2$ , available data provide few (if any) constraints on  $G(x, Q^2)$ , and cross section estimates are accordingly rather uncertain. This is illustrated in Ref. 5 by comparing rate predictions for two different choices of the gluon distribution at small  $Q_0$ :

$$xG(x, Q_0^2) \approx \text{const.}, \text{ for } x < 10^{-2}, \quad (4)$$

and

$$xG(x, Q_0^2) \approx 1/\sqrt{x}, \text{ for } x < 10^{-2} \quad (5)$$

for  $Q_0 = 5 \text{ GeV}$ . Eqs. (4) and (5) are each consistent with constraints from deep inelastic scattering data. For sufficiently large  $Q$  at any fixed  $x$ , QCD evolution ultimately washes out the effects of these different initial conditions. However, for bottom production with  $Q \approx 2M_b$ , the differences for evolution from Eqs. (4) and (5) are substantial, with Eq. (5) giving a total cross section through Eq. (2) which is more than three times as large as that arising from Eq. (4).

Heavy quarks produced by the fusion process in Eq. (1) have

$$p_T(Q) \approx M_Q. \quad (6)$$

For transverse momenta significantly larger than this value, the fusion mechanism is no longer the primary source of heavy hadrons. Instead the flavor excitation process in Eq. (3) and the production of heavy flavors in shower evolution of gluon jets,

$$g \rightarrow Q + \bar{Q}, \quad (7)$$

begin to dominate for  $p_T > M_Q$ . The UA1 group has examined single muon and dimuon production at the  $Spp\bar{S}$  and infer from

their measurements a (preliminary) cross section<sup>6</sup>

$$\sigma_{b\bar{b}} = 1.3 \pm 0.1 \pm 0.2 \text{ microbarn} \quad (8)$$

for

$$|y| \leq 2 \text{ and } p_T \geq 5 \text{ GeV}/c. \quad (9)$$

The gluon-gluon fusion expectation<sup>7</sup> is about 0.8 microbarn, with a possible factor of two uncertainty. The available data is thus consistent with substantial bottom production<sup>8</sup> occurring via the mechanism of Eq. (7).

The relative importance of various bottom production mechanisms at SSC is examined in Ref. 9. Figure 1 shows the total bottom production rates for  $p_T \geq p_T^{MIN}$  for the fusion, flavor excitation and shower evolution processes. The results in Fig. 1 were calculated using ISAJET.<sup>10</sup> Fusion is seen to be the largest single contribution to  $\sigma_{b\bar{b}}$  for  $p_T^{MIN} = 2 \text{ GeV}/c$ . For high  $p_T$  jets, the fusion mechanism is essentially negligible compared to bottom production in the shower evolution of gluon jets. It should be noted that the relative kinematic configurations of the  $Q$  and  $\bar{Q}$  are rather different for the fusion, flavor excitation and shower evolution mechanisms. Very crudely, fusion yields back-to-back  $Q$  and  $\bar{Q}$  jets; shower evolution gives  $Q$  and  $\bar{Q}$  rather close together in a single jet, and flavor excitation has a high- $p_T$   $Q$ -jet and a  $\bar{Q}$  "buried" in the beam remnants. Some initial investigations of the implications of these different kinematic configurations are contained in Ref. 9.

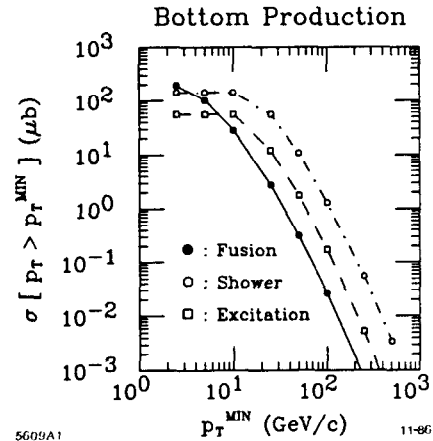


Figure 1 - The cross section for bottom production for  $p_T > p_T^{MIN}$  for the fusion, shower evolution, and flavor excitation processes as a function of  $p_T^{MIN}$ .

The production of heavy flavors during QCD shower evolution of gluon jets is in fact quite common. Figure 2 shows heavy flavor multiplicities in the shower evolution of  $gg$  systems of invariant mass  $Q$ . These results are calculated using a coherent parton shower model<sup>11</sup> and assuming  $M_t = 45 \text{ GeV}$ . The heavy flavor multiplicities per jet are half the values shown in this figure, and are consistent with the results given by Mueller and Nason.<sup>12</sup> Since

$$\frac{\sigma[gg \rightarrow gg]}{\sigma[gg \rightarrow Q\bar{Q}]} > 200, \quad (10)$$

it is clear from Fig. 2 that most heavy flavor production at high  $p_T$  has nothing to do with heavy flavor production in

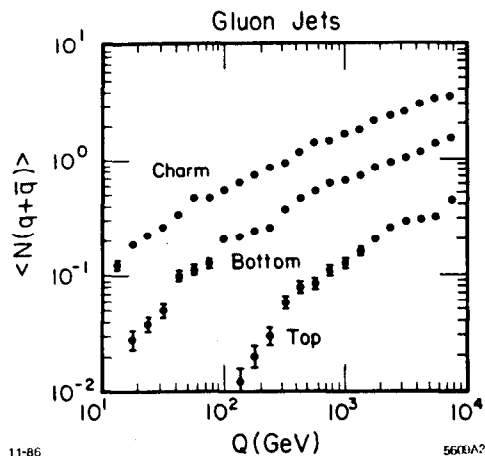


Figure 2 - Heavy flavor multiplicities<sup>11</sup> in the shower evolution of a gluon-gluon system of mass  $Q$ .  $M_t = 45$  GeV is assumed.

hard scattering subprocesses. Note that essentially all TeV gluon jets are expected to contain charm.

### 3. Flavor Tagging

The observation of displaced decay vertices is an effective technique for the tagging of charm and bottom which has been used successfully, particularly in charm studies at FNAL.<sup>2</sup> For the SSC, serious questions arise in regards to the survival of microvertex detection electronics in a high luminosity environment. This problem received considerable attention at Snowmass two years ago<sup>13,14</sup> and also during this meeting;<sup>15</sup> it will be taken up again in the last Section of this summary. The tentative conclusion of these studies is that some 'backing-off' in luminosity may be required to insure the survivability of the microvertex detector, typically from  $10^{33}$  down to  $10^{32}/\text{cm}^2$  sec. For now we set aside this 'technical difficulty' and consider the subsequent problems of using microvertex information for tagging bottom production.

At its design specifications, the SSC will produce  $b\bar{b}$  pairs at a rate which is several orders of magnitude greater than the rate at which events can be usefully recorded if they all were to be fully analyzed off-line. This fact is not necessarily a tragedy, in that it potentially allows the use of clever trigger and tagging strategies, using relatively rare  $B$ -decays, without the loss of 'useful' events for the physics issues in which one is interested. One such decay mode which was examined during the meeting is the decay chain

$$B \rightarrow \psi + X, \quad \psi \rightarrow e^+e^- \quad \text{or} \quad \mu^+\mu^- \quad (11)$$

This decay sequence is relatively easy to trigger on, as is discussed in more detail by Cox and Wagoner.<sup>15</sup> The presence of the  $\psi$  is particularly helpful in rejecting decay vertices arising from charm; only hadrons containing  $b$  quarks can have a  $\psi$  coming from a secondary vertex. The  $\psi$  decay to muon pairs in and of itself has the advantage of having a background primarily from directly produced  $\psi$ 's and is also sufficiently simple and isolatable to be useful in first-level triggering. With the TASTER detector described in the last Section (including a 12 GeV muon absorber) and a luminosity of  $10^{32}/\text{cm}^2$  sec, a net  $1.5 \times 10^7$   $b\bar{b}$  pair-containing-events are tagged by this method in a  $10^7$  sec experimental run according to the detailed Monte Carlo calculations in Ref. 15.

A different  $B$ -tagging scheme based on

$$B \rightarrow D^* \ell \nu + X \quad (12)$$

has been investigated by Panvini and Reeves.<sup>16</sup> This scheme requires the joint identification of the charged lepton in Eq. (12) and the daughter pion from the subsequent  $D^{*+} \rightarrow D^0\pi^+$  decays as coming from a secondary vertex. The low  $Q$  value in  $D^* \rightarrow D\pi$  decays assures us that

$$p_{D^*} \approx p_\pi (m_{D^*}/m_\pi) \quad (13)$$

provides a reasonable estimate of the momentum of the  $D^*$  in Eq. (12), and hence a (partial) reconstruction of the parent  $B$ . The inclusive branching ratio for the process in Eq. (12) is of the order of 5%. Allowing some reductions in tagging efficiencies due to various cuts made to clean up tagged events, this scheme could in principle possibly tag 1% of all  $B$ 's.<sup>16</sup> The technique proposed in Ref. 16 grew out of, and seems particularly promising for,  $e^+e^-$  annihilation. There, track multiplicities not associated with the  $B$  or  $\bar{B}$  are low or even non-existent, and event rates are low enough that high tagging efficiency is very desirable. Monte Carlo studies on the feasibility of this method for hadron-hadron colliders have only just begun.

At present, the most effective scheme for tagging top in high energy jets involves detection of isolated leptons from

$$t \rightarrow b \bar{\ell} \nu \quad (14)$$

semileptonic decays. This technique was investigated in detail by Lane and Rohlf<sup>17</sup> during Snowmass '84, and efficiencies of order 5 to 10% for top tagging were found. The isolated lepton analysis has now been repeated by Glover and Gottschalk,<sup>18</sup> using the improved version of ISAJET with initial state radiation.<sup>10</sup> While the changes in event simulation Monte Carlo models do not significantly reduce the effectiveness of top-tagging, the mass resolution for reconstruction of

$$X \rightarrow t\bar{t} \quad (15)$$

is found<sup>18</sup> to be somewhat worse than claimed in Ref. 17. This is simply a result of smearing due to the inclusion of occasional wide-angle bremsstrahlung of gluons from the initial state. Again, for  $p_\tau > MQ$  it is found that direct heavy quark production in the hard scattering subprocess is relatively unimportant compared with heavy flavor production in the shower evolution of gluon jets.

A simple attempt to separate direct and shower production of bottom in jets is presented in Ref. 19. The analysis is based on two rather general kinematic consequences of the splitting in Eq. (7):

1. The bottom hadron energy spectrum from Eq. (7) is rather softer than that from hadronization of bottom jets.
2. The energy flow in gluon jets is significantly more spread out than in quark jets.

The first point is illustrated in the top half of Fig. 3 where distributions in  $dN/dz_x$  for bottom mesons in  $b$ -jets (points) and gluon jets (histograms), for jets with  $p_\tau \approx 200$  GeV are presented. The curves are individually normalized to the bottom multiplicity per jet; the  $g \rightarrow B$  results should accordingly

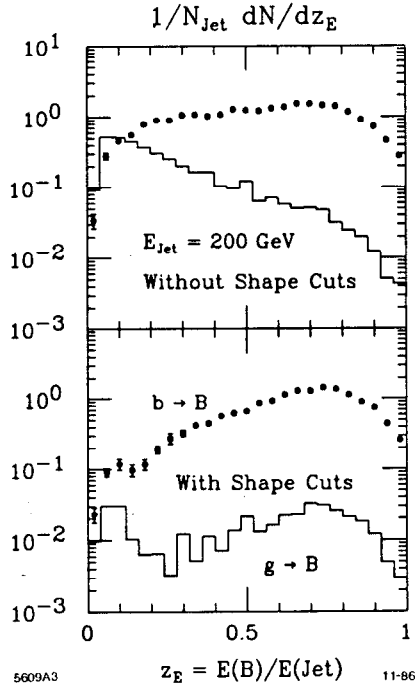


Figure 3 - The distribution  $dN/dz_E$  for bottom mesons in  $b$ -jets (points) and in gluon jets (histogram) for jets with  $p_T = 200$  GeV and without (upper) and with (lower) shape cuts on the energy distribution in the jet.

be scaled up by about a factor of 200 to give a true indication of signal:background.

The second point can be utilized to further isolate  $b$  quark jets by making simple cuts on the "shape" of jets. The analysis in Ref. 19 first defines jets using a UA1-like jet finding algorithm<sup>20</sup> with

$$\Delta R = [(\Delta\eta)^2 + (\Delta\phi)^2]^{1/2} > 1. \quad (16)$$

Given the jet axis and jet energy from this first step, the fraction  $f_\Delta$  of the total  $E_T$  contained in a cone with  $\Delta R = 0.4$  is calculated, and an additional cut  $f_\Delta > f_0$  is imposed. The bottom half of Fig. 3 shows the effects of a cut  $f_\Delta > 0.8$ . In this particular example, the shape cut and a cut  $z_E > 0.3$  can reduce the background from Eq. (7) by more than an order of magnitude while accepting almost 70% of the prompt  $b \rightarrow B$  events. Without much effort at optimization, signal to noise rates of order 1:4 are easily achieved.<sup>19</sup>

#### 4. New Physics Investigations Using Heavy Flavors

A central fixture of SSC physics discussions is the Higgs boson. For Higgs masses below about 80 GeV, its discovery is likely before the SSC era at the SLC, LEP I, or LEP II. For masses above this but below  $2M_W$ , the so-called "intermediate mass" Higgs, the dominant decay mode is to the most massive quark-antiquark pair allowed by phase space.

At the 1984 Snowmass meeting the possibility of detecting a Higgs boson decaying to top quarks at the SSC was evaluated.<sup>21</sup> The overall prognosis for Higgs detection was gloomy, particularly after cuts were made to reduce very high backgrounds, jet reconstruction ambiguities were taken into account, and detector resolution folded in. Semileptonic decays involving missing neutrinos gave rise to substantial low

mass tails to the reconstructed Higgs mass peak, and signal to background in the mass band around the peak was about 0.04.

At this meeting the subject has been re-opened in the form of an examination of the possibilities of detecting a Higgs boson decaying to bottom quarks.<sup>22</sup> This was motivated by several things that have happened in the past couple of years. First, our level of certainty about the  $t$  quark mass has decreased; at this time it is still quite possible that the  $t$  quark is heavier than  $M_W$ . Second, the Monte Carlo programs to generate both signal and background events have very much improved. Third, additional ideas and corresponding algorithms to enhance and/or separate heavy quark jets from jets due to light quarks or gluons have been developed, as discussed in Section 3. Finally, the possibility that  $H \rightarrow b\bar{b}$  might be the decay mode of choice for detecting the intermediate mass Higgs seems likely to improve the signal to background ratio. This is so because a) background processes containing  $\bar{b}c$  combinations where the  $c$  is mistaken for a  $b$  are suppressed by KM angles (unlike the situation for  $H \rightarrow t\bar{t}$ , where  $\bar{b}t$  with the  $\bar{b}$  mistaken for a  $\bar{t}$ , proved a very serious background<sup>21</sup>); and b) the long  $b$  lifetime gives the opportunity for identification of  $b$  quark jets by means of secondary vertices that would not be available for  $t$  jets.

The investigation of detecting the Higgs boson decaying to  $b\bar{b}$  was undertaken with the PYTHIA Monte Carlo program<sup>23</sup> to generate both signal and background events, with the signal events being 'tagged' by an accompanying  $W$  or  $Z$ :

$$pp \rightarrow H^0 + (W \text{ or } Z) + X \quad (17)$$

The signal for  $b$  jets was enhanced, and the background from gluon jets decreased by requiring that (1) one of the two jets contain a lepton with a transverse momentum relative to the jet axis of greater than 1 GeV, and (2) that both jets satisfy a cut<sup>19</sup> that 70% of their energy lie in a cone of  $\Delta R < 0.5$ . These cuts bring the signal to background ratio to 0.8 in the rather broad Higgs mass peak region. While not conclusive, especially because the resulting signal of about 2,000 events for an integrated luminosity of  $10^{40}/\text{cm}^2$  is not enormous, this is considerably more encouraging than the case when  $H^0 \rightarrow t\bar{t}$ , and indicates that it merits further study both with a central detector and a semi-forward one.

Another subject of great physics interest is the possibility of tagging continuum  $W$ -pair production,

$$q + \bar{q} \rightarrow W^+ + W^- \quad (18)$$

This is investigated through use of the decay chain

$$W^+ \rightarrow \mu^+ \nu_\mu, W^- \rightarrow b \bar{c} \rightarrow b \bar{b} \mu^- \nu_\mu \quad (19)$$

and its charge conjugate in Ref. 24. ISAJET events for both Eq. (19) and the single- $W$  QCD backgrounds,

$$q + \bar{q}' \rightarrow W + g, \text{ etc.} \quad (20)$$

are examined for  $p_T(W) \approx 100$  GeV. Initial event selection cuts

$$p_T(\mu_2) > 10 \text{ GeV} \quad (21)$$

$$p_T(\mu_1) - p_T(\mu_2) > 20 \text{ GeV} \quad (22)$$

$$E_{\text{CONE}}(\mu_2, \Delta R = 0.4) < 15 \text{ GeV} \quad (23)$$

provide a useful trigger for Eq. (19) while eliminating (essentially) all QCD backgrounds except for top production in the

recoil jet in Eq. (20). In Ref. 24, the muon with the largest  $p_T$  is simply assumed to come from  $W \rightarrow \mu\nu$  decay. With the additional selection cut in Eq. (22), this assignment is found to be correct about 90% of the time.

The cuts in Eqs. (21)–(23) give an acceptance of about 25% for Eq. (19) and about 0.2% for the background in Eq. (20). The signal-to-noise level at this stage in the analysis is about 1:70. Several additional cuts are then imposed to reduce the background level. A transverse mass  $M_T(\mu_1, p_{T-MISSING})$  is constructed using the muon with largest  $p_T$  and the total missing transverse momentum in the event. The additional neutrino from top decay distorts, but does not destroy, the expected peak in the transverse mass distribution, as seen in the top half of Fig. 4. Candidate  $W \rightarrow \mu\nu$  events are selected by a cut,  $35 \text{ GeV} < M_T < 140 \text{ GeV}$ . Next, jets near the muon ( $\mu_2$ ) with lower  $p_T$  are found using a simple jet finding algorithm, and a cut,  $55 \text{ GeV} < M < 80 \text{ GeV}$ , is imposed on the  $M(\mu_2, \text{jet}, \text{jet})$  mass distribution shown in the bottom half of Fig. 4. Finally, the net transverse momentum of the reconstructed  $WW$  system was required to be less than 20 GeV.

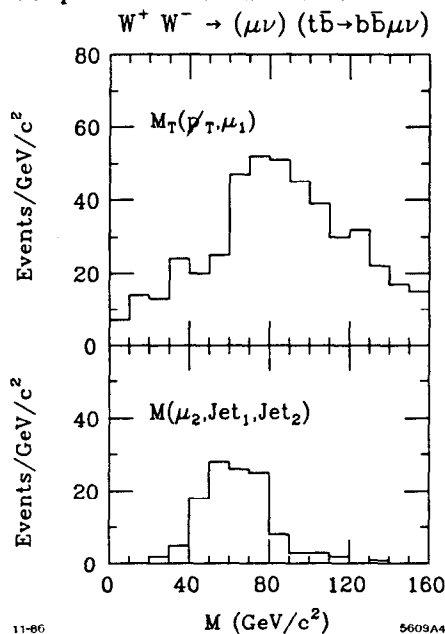


Figure 4 - Reconstructed mass distributions for  $W$  pair production where one  $W$  decays to  $\mu\nu$  and is reconstructed from an observed muon and  $p_{T-MISSING}$  (upper histogram) and the second  $W$  decays to  $b\bar{l}$ , followed by semileptonic decay of the  $\bar{l}$ , and is reconstructed from the second muon and two ( $b$  containing) jets (lower histogram).

The conclusions of Ref. 24 are encouraging when compared to that of the Heavy Higgs group at the UCLA meeting<sup>25</sup>, which concluded that no cuts could be found to separate the signal in Eq. (19) from the background in Eq. (20) for hadronic  $W$  decays into light flavors. With the additional top tagging, the identification of Eq. (19) is apparently possible (albeit barely). It is still discouraging, however, that in one SSC year at full luminosity one is left using this method with 20 events of the type in Eq. (19), together with a residual QCD background of about 80 events!

The possibility of detecting a fourth generation, charge  $-1/3$  heavy quark,  $\nu$ , at the SSC is investigated in Refs. 26 and 28. In both these works, the  $\nu$  quark is assumed to decay

into top plus a real  $W$ , and the production/decay sequence

$$g + g \rightarrow \nu + \bar{\nu} \rightarrow (t W^-) + (\bar{l} W^+) \quad (24)$$

is investigated. The total cross section for this process is quite large, typically 3000–500 pb for  $M_\nu \approx 200 - 500 \text{ GeV}$ .

Reference 26 investigates the scenario in which one of the  $W$ 's in Eq. (24) decays leptonically, and both  $t$ 's and the other  $W$  decay into hadronic jets. The analysis in Ref. 26 is based on very high statistics ISAJET simulations, with 100K events for Eq. (24) as well as 100K events for the background process of continuum  $W$ -pair production. Given this large 'event' sample, the analysis procedure essentially involves stringent mass cuts for pairs of jets reconstructing to  $t$ 's or  $W$ 's. As a typical example, events with a reconstructed leptonic  $W$  decay and six distinct hadronic jets are examined! Next, pairwise combinations of jets are formed and identified with a  $W$  or  $t$  if  $65 \text{ GeV} < M < 105 \text{ GeV}$  or  $30 \text{ GeV} < M < 50 \text{ GeV}$ , respectively. Finally, in events with two tagged  $W$ 's and 2 tagged  $t$ 's, the  $t \leftrightarrow W$  pairing which gave the more nearly equal masses for the reconstructed  $\nu$ 's was chosen. The resulting signal is impressive and the background from continuum  $W$ -pair production is shown to be negligible.<sup>26</sup> This success relies on the severe cuts used to identify hadronic top and  $W$  decays. Only 0.4% of the total event sample for Eq. (24) survives the cuts imposed. The weakness of this analysis is in the background estimates and the associated question of triggering. The initial event selection criteria require only a charged lepton with  $p_T > 25 \text{ GeV}$  and at least 25 GeV of missing transverse momentum. For these cuts, single- $W$  production as in Eq. (20) will be an overwhelming background and cause serious problems at the trigger level.<sup>27</sup>

Some initial attempts to deal with the trigger and background problems surrounding Eq. (24) are presented in Ref. 28. As a specific signature for the process in Eq. (24), events are selected with two isolated, high- $p_T$  charged leptons on the same side, corresponding to leptonic  $W$  decay and semileptonic  $t$  decay of the daughters of a single heavy quark. Reconstruction of the  $\nu$ -quark mass is then done by examining various jet mass combinations on the other side of the event (the transverse momentum of the most energetic lepton in the trigger provides an axis for the specification of "same" and "opposite" sides). To avoid contamination from obvious sources of isolated, high- $p_T$  lepton pairs (e.g.,  $Z$  or  $\gamma^*$ ), the charged leptons in the trigger can be required to have different flavors. In order to have any sensible separation of same-side and opposite-side jets, the algorithm in Ref. 28 must be restricted to events with  $p_T(\nu) > M_\nu$ . This high- $p_T$  selection provides further background suppression.

The Monte Carlo event sample used in the calculations of Ref. 28 was rather small (about two orders of magnitude fewer events than in Ref. 26), and the reconstructed mass distributions shown in Ref. 28 are accordingly somewhat marginal. The results in Ref. 28 (and presumably in Ref. 26 as well) are found to be rather sensitive to details of the jet finding algorithm used in the analysis. While neither of the  $\nu$ -quark studies is conclusive, it seems plausible that some combination of the techniques used in these works can allow detection of the process in Eq. (24) for  $\nu$ -quark masses up to a few hundred GeV.

## 5. Rare Decays and CP Violation in the $B$ Meson System

The promise of interesting physics in the  $B$  meson system is very tempting. In particular, there are specific decay modes of the neutral  $B$  mesons within which one expects CP violating asymmetries at the several percent level in the standard model. Not only does one have the prospect of observing CP violation outside the neutral  $K$  meson system, its only observational place until now, but the magnitude of the asymmetry is in some cases much larger than  $|\epsilon_K|$ , providing a pattern characteristic of the standard model as distinguished from other explanations of CP non-invariance.

However, the  $B$  meson branching fractions or mixing rates times branching fractions that go with the "big" asymmetries are very small, typically from  $10^{-4}$  to  $10^{-7}$ ! That is where the SSC comes in, for only at the SSC can one clearly envision  $B$  meson production at a level so as to make some of these experiments feasible even in principle. The main experimental problem is of course to fish out a large enough sample of  $B$  decays in the appropriate channels. This is the subject of the next Section. But first we need to know what specifically are the appropriate channels and what are their branching ratios?

This was re-examined at this meeting in the light of the current experimental situation for  $B$  decays and theoretical insights over the past couple of years.<sup>29-32</sup> There still are considerable uncertainties in many of the calculated rates. It is important to bear this in mind and to consider both as large a spectrum of processes of interest as possible together with the corresponding range of theoretically predicted rates in order to get a rough idea of what the physics potential of the SSC might be. Needless to say, even a few crudely measured branching ratios for rare  $B$  decays would serve to tie down the theoretical calculations and allow much more incisive predictions of which specific processes it is best to concentrate on and what level of statistics is needed to realize a significant measurement.

Rare  $B$  decays like  $B \rightarrow K\mu^+\mu^-$  and  $B \rightarrow K^*\gamma$  are expected at the  $10^{-6}$  level in branching ratio.<sup>29</sup> They are a kind of benchmark for this type of physics, as they are expected in the standard model through one loop ("electromagnetic penguin") diagrams. The branching ratio for the former is insensitive to the  $t$  quark mass; that for the latter depends rather strongly on it.

Related, but less certain, are the rates for processes involving "penguin" diagrams with gluons. Examples are  $B_d \rightarrow K\phi$ ,  $B_s \rightarrow \phi\phi$ , etc., which likely have branching ratios in the neighborhood<sup>29</sup> of a few times  $10^{-5}$ . As we will discuss shortly, the presence of these diagrams is important in a number of decay channels where it is possible to look for CP violation.

There are also rare  $B$  decays that do not depend on "penguins" like  $B \rightarrow \tau\nu$  and  $B \rightarrow \gamma\gamma$ . The former process is proportional to the rate for the  $b \rightarrow u$  transition. It also is expected<sup>29</sup> at the level of a few times  $10^{-5}$  or so.

Much more interesting if they are found, because they must originate beyond the standard model, are decays such as  $B \rightarrow \mu\tau$  or  $B \rightarrow K\mu\tau$  which involve flavor changing neutral currents. There is a wide range of possible predicted rates, depending on the model and, more specifically on the couplings and mass of the particle whose couplings change flavors. It is possible to envision<sup>29</sup> branching fractions as big as "standard model" rare modes, i.e. a few times  $10^{-5}$ ; it also is possible in the same

kinds of models to push these branching ratios down below  $10^{-9}$ . Of course, at the moment, nothing demands a departure from the standard model where these processes are forbidden.

Turning to CP violation in the  $B$  meson system, there are several different avenues for its experimental investigation. The most direct extension from what we are familiar with in the neutral  $K$  system is to look for CP violation in the  $B^0 - \bar{B}^0$  mass matrix. The standard avenue is to look for a charge asymmetry in  $B^0$  semileptonic decays, in particular, a non-zero value of the quantity

$$\alpha_{\text{semileptonic}} = \frac{N(\ell^+\ell^+) - N(\ell^-\ell^-)}{N(\ell^+\ell^+) + N(\ell^-\ell^-)} \quad (25)$$

when both  $B$ 's in a  $B^0 - \bar{B}^0$  system decay semileptonically. This requires both the presence of  $B - \bar{B}$  mixing and CP violation. Estimates based on the standard model indicate values of  $\alpha_{\text{semileptonic}} \approx 10^{-3}$  and a few percent mixing for  $B_d$ , so that more than  $10^{10}$   $B - \bar{B}$  pairs are needed for a 3 standard deviation effect.<sup>32</sup> The  $B_s$  case is no better. This is not the optimal place to look first, unless non-standard model physics intervenes.

A more optimistic situation is encountered by considering nonleptonic decays with a final state that is common to both  $B$  and  $\bar{B}$ . Again mixing is essential to obtaining a non-vanishing difference between the decay rate for a  $B$  and a  $\bar{B}$ , even if CP violation is present. One may also look for a proper time dependence in the decay of a  $B$  or  $\bar{B}$  to the common final state. In either case it is necessary to know if one starts with a  $B$  or a  $\bar{B}$ , i.e. one needs to tag either from knowledge of the parentage of the decaying particle or knowledge of the accompanying  $\bar{B}$  or  $B$ . Typical decay modes are generated at the quark level from  $b \rightarrow c \bar{c}d$  and show up in exclusive channels like  $B_d \rightarrow \psi K_S$ ,  $B_d \rightarrow D\bar{D}$ , and  $B_s \rightarrow \psi\phi$ . Their branching ratios are probably at the  $10^{-3}$  level,<sup>29-32</sup> but could be larger in particular cases. The projected asymmetries on the other hand, could well be fairly large, from a couple percent up to 20 percent.<sup>29-32</sup>

A final class of CP violating asymmetries can arise without the presence of mixing, but with different final state interactions for two (or more) contributions to the same final amplitude. Such asymmetries in decay rates between a particle and an antiparticle can arise as true interferences at the hadron level between two cascade chains to the same final state, or at the quark level as an interference between spectator and annihilation or spectator and "penguin" contributions to the full amplitude. Examples are to be found in neutral  $B$  decays such as  $B_d \rightarrow K^+\pi^-$  and its charge conjugate, but also for charged  $B$  decays such as  $B_u \rightarrow K^+\rho^0$  and its charge conjugate. Here one has the big advantage that tagging the nature of the decaying  $B$  is not necessary; it signs its own name (whether a  $B$  or  $\bar{B}$ ) through its decay products. The difficulty arises from small branching ratios of  $10^{-6}$  up to a few times  $10^{-5}$  for typical cases,<sup>29-32</sup> and small to moderate asymmetries of 1 to 10 percent.<sup>29-32</sup> The calculations are particularly uncertain because they involve, for example, the interference of spectator and penguin diagrams with different Kobayashi-Maskawa factors and matrix elements.

Even with these uncertainties, it seems better to look at processes with very small branching ratios, but potentially larger asymmetries. Thus we concentrate on a few examples of

this type in the next Section when we explore the capabilities of the TASTER to do this type of physics.

### 6. The TASTER: A Detector for Studying $B$ Decays

During the course of the discussions which took place in the Heavy Flavor Working Group, many of the participants reached the conclusion that the physics of  $B$  decays (and in particular the rare and CP violating decays) was of sufficient interest to merit a dedicated, specially designed detector and interaction region at the SSC. Such a detector, with the capability of detecting and reconstructing hadrons containing bottom quarks, could also be used to search for heavier generations of quarks which decay into bottom. A detector which was specially designed to maximize the collection of  $B$  decays would be quite different in configuration from the generic  $4\pi$  detector.

The detector configuration dubbed the "TASTER" and shown schematically in Figure 5 is a beginning of a design which is optimized for the collection of bottom decays. The elements of the detector as well as its overall configuration are dictated by the dynamics of the dominant mechanism for beauty production at  $\sqrt{s} = 40$  TeV,  $gg \rightarrow b\bar{b}$ , and by the requirement of complete reconstruction of the  $B$  meson or baryon from its decay products.

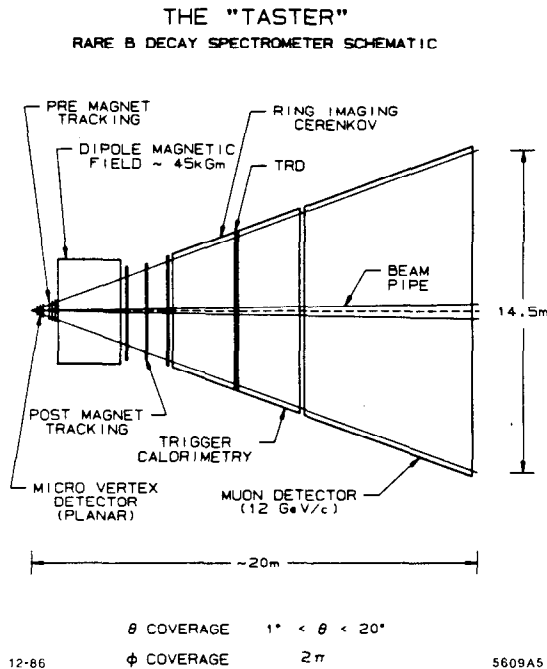


Figure 5 - Schematic representation of the "TASTER" detector

References 5, 7, and 15 have investigated the features of gluon fusion production of  $b\bar{b}$  final states at SSC energies and have found several striking features. First, the majority of the  $b\bar{b}$  production is at low transverse momentum. Any experiment that attempts to accumulate large numbers of  $B$  decays must detect low transverse momentum  $B$ 's. Second, the  $B$ 's (and, therefore, their decay products) have relatively low momentum, comparable to TEV II fixed target experiments. This leads to problems for the detector both in preparing proper triggers and in separation of the  $B$  decay products from the backgrounds due to events which make up much of the total cross section. Third, the momentum of the  $B$ 's are highly correlated with the production angle of the  $B$ 's. The only region

which contains  $B$ 's with appreciable momentum is the forward region along either beam direction. Finally, there is a strong correlation of the  $b$  and the  $\bar{b}$  directions. They are preferentially produced with both the  $b$  and the  $\bar{b}$  emitted along the beam direction (see Fig. 3b of Ref. 15). The most fruitful region for collecting both the  $b$  and the  $\bar{b}$  simultaneously is the angular region below 20 degrees, where the angle is measured with respect to either beam direction. In fact, approximately 25% of the  $b$  and  $\bar{b}$  quarks are emitted into the same 20 degree angle along a given beam direction. The acceptance for  $b\bar{b}$  pairs can thus be doubled by constructing two detectors, one along each beam direction.

These features make it possible to plan for a heavily instrumented detector which covers only the forward regions along one or the other beam directions. The coverage of a limited solid angle additionally permits one to consider complete particle identification and reconstruction, which is necessary for exploring many facets of the physics of  $B$  decays and which would be hard to accomplish over the entire  $4\pi$  solid angle. The extreme forward region, below one degree, is not covered. Such coverage would produce a limited increase in statistics because of the rapidly falling production cross sections at large rapidities. The additional expense and the increase in technical problems that would be incurred by attempting such coverage was thought not to be worth the relatively moderate increase in statistics that could be gained.

A beginning was made during the Heavy Flavor Working Group sessions in considering the serious problems that a detector, configured as above, and attempting to go down to relatively low momentum to collect as many  $b\bar{b}$  decays as possible, will encounter in trying to sort out the desired signals. The large multiplicities of SSC events (see Figures 6a and 6b) and the high operating luminosities present particular problems both in sorting out the response of various components and in the level of radiation damage that each component must withstand. Some of these issues are discussed and a few conclusions drawn in what follows below.

Discussions of the maximum rate at which such a forward detector could operate, like previous discussions at earlier workshops, were somewhat inconclusive. However, unlike some experiments which, for example, will search for high  $p_T$  phenomena selected by calorimetric triggers, an experiment which seeks to maximize the number of  $b\bar{b}$  pairs that are completely reconstructible may not be able to operate at the maximum luminosity available at the SSC ( $10^{33}/cm^2 sec$ ) simply because of the limitation on the number of  $b\bar{b}$  events that can be recorded. The Offline Computing Group at the Fermilab Triggering Workshop<sup>33</sup> considered a logging rate of a few events per second with a megabyte per event to be a feasible data acquisition capability that experiments should plan for at the SSC. At a reduced luminosity of  $10^{32}/cm^2 sec$  the expected inelastic  $pp$  total cross section of 100 mb will lead to  $10^7$  interactions per second. Out of this, a few events per second can be logged. The  $b\bar{b}$  cross section itself is expected to be<sup>3-5,7,9,34</sup> 200 to 400 microbarns, leading to 2 to  $4 \times 10^4$   $b\bar{b}$  pairs produced per second! Because of the restrictions on the data logging rate, perhaps only 10 (at most, probably 100 events) can be recorded per second even if a trigger that was perfectly selective for the signal could be constructed.

Therefore, it is likely that the operating luminosity for the TASTER will be limited by the saturation of the data acquisi-

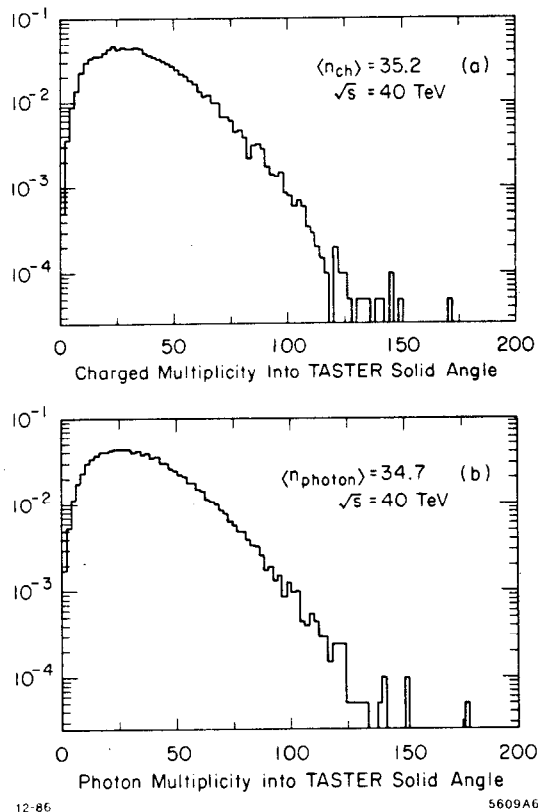


Figure 6 - The total charged multiplicity (a), and the corresponding photon multiplicity (b), as predicted by PYTHIA into the solid angle of the TASTER detector.

tion rate with a given trigger strategy. At present a luminosity of  $10^{32}/\text{cm}^2 \text{ sec}$  seems more than enough to saturate the data collection rate even if the rather selective dimuon trigger strategy discussed in Ref. 15 is used. Other trigger strategies may still be unearthed that require the maximum luminosity that is potentially available at the SSC, but at the present the  $b \rightarrow \psi + \dots \rightarrow \mu^+ \mu^- + \dots$  trigger seems to offer the best opportunity for triggering and tagging a clean sample of  $b$  decays. If data acquisition systems with more capability can be constructed, operation at luminosities greater than  $10^{32}$  may become possible, but other problems such as radiation damage (which is already serious at  $10^{32}$ ) may become the ultimate limitation.

Therefore, since the TASTER may be limited by data acquisition and logging capabilities, trigger strategies which sacrifice  $b\bar{b}$ 's for purity of the data sample can be entertained. In particular, the authors of Ref. 15 have investigated the feasibility of a trigger on  $\psi \rightarrow \mu^+ \mu^-$ , where the  $\psi$ 's come from the decay of  $B$  mesons with a 1.1% inclusive branching fraction. The presence of a  $\psi$  at a secondary vertex also unambiguously tags the event as having a  $b$ . Their conclusion is that the total trigger rate at a luminosity of  $10^{32}/\text{cm}^2 \text{ sec}$  into the solid angle for a TASTER-like detector for muon pairs due to pion decays, pion punch through, directly produced  $\psi$ 's and the signal itself is fairly consistent with the data acquisition and logging rates ( $10^1 - 10^2/\text{sec}$ ) expected to be available for SSC experiments. This dimuon trigger (see below) will preserve an acceptable fraction ( $\sim 5\%$ ) of the signal for  $b \rightarrow \psi + \dots \rightarrow \mu^+ \mu^- + \dots$ , which is the process of interest. When the requirements that the muon pair arise from a  $\psi$  and that the  $\psi$  come from a

secondary vertex are imposed offline, a huge rejection against the various backgrounds from charm decays and from other muon pair sources is achieved, since no mechanism other than bottom decays can produce a  $\psi$  at a secondary vertex.

The major offline background to a  $B$  data sample obtained by this strategy is due to mismeasured directly produced  $\psi$ 's which appear to be coming from a secondary vertex. The average separation of the secondary vertex from the primary vertex in the dimensions transverse to the beam direction is 170 microns because of the relatively long lifetime ( $\sim 1.2 \times 10^{-12}$  seconds) and the average  $p_T$  ( $\sim 6.5 \text{ GeV}/c$  according to PYTHIA) of the  $b$  quarks. These decay flight paths are long enough that the microvertex detector discussed below should have relatively little problem in resolving  $B$  decay secondary vertices from primary vertices because of the expected good resolution for reconstructing vertex positions in the transverse plane. Since the ratio of  $\psi$ 's from  $b \rightarrow \psi$  to directly produced  $\psi$ 's has risen at  $\sqrt{s} = 40 \text{ TeV}$  to 3:1, the rejection of directly produced  $\psi$ 's need only be rather modest. It seems completely feasible even with the lower resolution of a microvertex detector placed relatively far from the interaction point (as is the case at the SSC, because of radiation damage and the finite size of the beam intersection region,  $\sim 7 \text{ cm}$ ) to achieve rejection of directly produced  $\psi$ 's of better than  $10^{-2}$ . Therefore, the dominant background considered thus far appears to be completely negligible.

Other strategies for tagging  $B$  decays involving semileptonic decays of the  $B_d$  have been discussed (such as the decay  $B_d \rightarrow D^+ \ell + \nu + X$  discussed in Ref. 16). These strategies are interesting as a tag of a  $B$  decay, but the trigger rates encountered when attempting to separate the  $b\bar{b}$  events from the backgrounds due to pion decay (for the muons) and photon-hadron overlaps (for electrons) in high multiplicity SSC interactions are likely to be large. This fact makes it unlikely that semileptonic decays can be effectively used as a trigger. The trigger rates in question have yet to be studied in detail. In addition, while the numbers of  $B_d$  semileptonic decays produced in various channels are large because of relatively large branching ratios, the effects of the various cuts necessary to get a clean sample of single leptons and pions (in the vicinity of a jet) have not yet been completely calculated. Finally, the complete reconstruction of the  $B$  hadron is manifestly impossible in a decay mode in which a neutrino is present, so many kinds of  $B$  physics are precluded if semileptonic modes are used. Further study is needed to ascertain the potential of this tag in the environment of high multiplicity hadron-hadron interactions and multiple charm production.

The components which a spectrometer designed to accumulate  $b\bar{b}$  pairs and completely reconstruct their decays should have are indicated in the schematic drawing of the detector (Fig. 5). These elements are briefly discussed below:

#### A. Silicon Microstrip Detector

A planar microvertex detector covering the  $1^\circ < \theta < 20^\circ$  solid angle of the TASTER is an absolutely essential component of a detector constructed to study bottom since an outstanding characteristic of  $b$  hadrons is their long lifetime. As discussed above, the TASTER must be capable of detecting the secondary vertices produced by such decays. This microvertex detector should be placed as close to the interaction region as possible in order to maximize the resolution in the transverse



position of the secondary vertex while still allowing the detector to survive the radiation damage at  $10^{32}/\text{cm}^2 \text{ sec}$  luminosity for  $10^7$  seconds (a canonical one year run). The radiation damage criteria would dictate that we position the microvertex detector as far from the interaction region as possible. A positioning of 20 cm from the center of the interaction region, while not completely optimum, has been used for the purposes of this study. This detector is presently thought to be composed of 12 planes of 300 micron silicon ruled into 25 micron strips in three modules ( $x$ ,  $x'$ ,  $u$ , and  $v$  orientations separated by 10 cm). The number of planes one can use is limited by the fact that, among other things, the silicon represents an appreciable fraction of an interaction length for all of the secondaries combined.

With a microvertex detector positioned at 20 cm from the center of the interaction region, resolutions on the transverse positions of the secondary and primary vertex of better than 25 microns should be possible. As can be seen from Figs. 7a and 7b, the distances which the  $b$  hadrons travel before decaying in the forward solid angle for an SSC experiment are large compared to the estimated  $\sigma_{x,y} \sim 25$  micron resolution for a planar microvertex detector covering the  $1^\circ < \theta < 20^\circ$  solid angle of the TASTER.

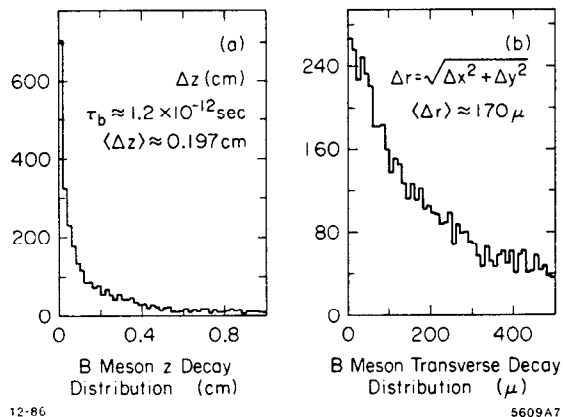


Figure 7 - The distribution of the distances (in cm) of the bottom decay vertices relative to the production point for a  $b$  lifetime of  $1.2 \times 10^{-12}$  seconds (a) in the direction along the beam, and (b) in  $\Delta r$  in the plane perpendicular to the beam direction.

At that distance from the interaction region, radiation damage is a serious problem. We have left a 2 mm radius hole in the center of the silicon detector planes, both to allow the unimpeded passage of the beams ( $\sigma \sim 7$  microns) and also to minimize the radiation damage in the central strips. At 20 cm distance from the center of the interaction region, this hole represents a 0.5 degree aperture, so we have a more than adequate match to the  $1^\circ < \theta < 20^\circ$  coverage of the rest of the detector. Figure 8 shows the radiation damage integrated over each 25 micron strip for a 20 cm positioning of a detector with such a hole in the silicon planes. We have expressed the radiation in terms of dosage per 25 micron strip, since radiation damage to a silicon detector is apparently manifested<sup>35</sup> as an increase in electronic noise until a minimum ionizing signal is buried in the noise, rather than any diminishing of the signal level itself. Therefore, any radiation problem should be proportional to the integrated radiation dose on a given strip. The 100 or

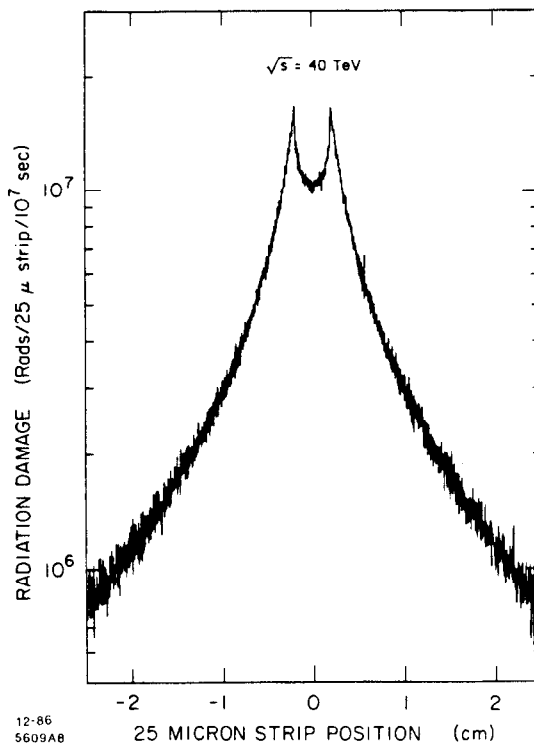


Figure 8 - Radiation damage expected to be suffered in a year of operation ( $10^7$  sec) at a luminosity of  $10^{32}/\text{cm}^2 \text{ sec}$  in the TASTER silicon detector positioned 20 cm from the center of the SSC interaction region.

so strips in the central region of the microvertex detector experience damage at a level between  $10^6$  and  $10^7$  rads per year in this configuration.

This level may be acceptable, although few measurements are available. If not, two possible solutions are: move the silicon detector back from the interaction region (thereby decreasing the transverse spatial resolution on secondary decay vertices and, therefore, the background rejection) or, consider cumbersome (but conceivable) mechanical systems in which the central 100 strips of each plane can be remotely changed every few days without breaking the machine vacuum.

#### B. Pre-Magnet Tracking System

This is a system of relatively standard PWC's with wire spacings of 1.5 to 2 mm. The main purpose of this system is to allow the measurement of  $K_S^0$ 's produced in the  $b$  decays. Since normally the  $K_S^0$ 's will decay beyond the microvertex detector, some additional measuring capability is necessary upstream of the magnet. The most serious difficulty with this system is the operation at high rates.

#### C. Analysis Magnet

This is a relatively simple 45 kG-m integral  $B \cdot dl$  dipole magnet for momentum analysis of charged tracks. Without extensive Monte Carlo estimates, we have judged from previous experiments that mass resolutions for systems of charged particles quite a bit better than  $50 \text{ MeV}/c^2$  (sufficient to resolve purely charged particle decays of the  $B_d$  from those of the  $B_s$ ) should be possible with such a magnet. This mass resolution will be considerably improved by use of the trick of fixing the dimuon mass to  $3.097 \text{ GeV}/c^2$  for those events found to be in the  $\psi$  peak.

#### D. Post-Magnet Tracking System

This straight-forward system consists of an adequate number of PWC's (with 2 mm wire spacings) to provide post-magnet trajectory information on charged tracks before and after the ring imaging counter.

#### E. Ring Imaging Cerenkov Counter

This highly segmented device is essential for the complete reconstruction of the final states of the  $B$  decays. In particular, the reconstruction of  $B_s$  and  $B_d$  mesons will be ambiguous unless good  $K - \pi$  identification can be achieved over a considerable kinematic range. However, due to the moderate momentum of  $K$ 's and  $\pi$ 's from both  $b$  decays and from backgrounds, good identification of  $K$ 's can be achieved using a relatively short ring imaging Cerenkov counter.<sup>36</sup> Figures 9a and 9b show the momentum spectrum of  $K$ 's from  $b$  decay and those from events making up the total cross section, respectively. We note that  $K$ 's are so numerous in events composing the total cross section ( $\langle n_K \rangle \approx 3.1$  per event into the solid angle of the TASTER), that they will provide no special signature for a  $b$  trigger. Therefore, there is no premium on the fast extraction of information from the Cerenkov detector. Reference 36 discusses a particular model of this device which is suitable for the TASTER. The problems of developing algorithms to sort out the rings in such high multiplicity events has been studied in Ref. 36 with relatively positive results.

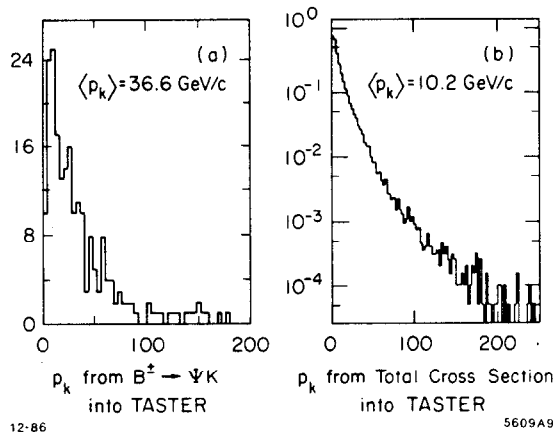


Figure 9 - Momentum spectrum of  $K$ 's into the TASTER solid angle from (a)  $B_u^\pm \rightarrow \psi K^\pm$ , and from (b) total cross section events.

#### F. Transition Radiation Detector

This device is included for additional electron identification beyond that possible in the calorimeter. This is particularly useful for identification of the decay products from semielectronic decays of  $B$ 's. It is anticipated that an additional suppression of pion contamination in the electron signal by a factor of 10 to 50 can be achieved in the momentum range appropriate for semielectronic decays of  $B$ 's into the TASTER solid angle (see Fig. 10a) using TRD techniques already developed at the present time.

#### G. Electromagnetic and Hadronic Calorimetry

The primary use of this calorimetry is electron-pion separation by an  $E$  (from calorimeter)/ $p$  (from magnetic analysis) calculation and formation of additional triggers designed to insure high momentum electrons in the trigger sample. The preliminary estimate is that a 24 radiation length electromagnetic

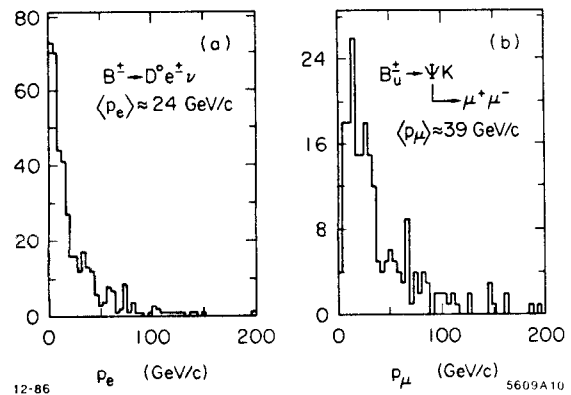


Figure 10 - The momentum spectra within the TASTER solid angle of (a) electrons from the semileptonic decays  $B_u^\pm \rightarrow D^0 e^\pm \nu$ , and of (b) muons from the decay  $B \rightarrow \psi K \rightarrow \mu^+ \mu^- K$

detector and a total of 9 interaction lengths for the hadronic detector will be adequate for the needs of the TASTER. No special techniques will be necessary for the hadronic detector since neither hermeticity (obviously) nor extraordinary energy resolution is being contemplated for the TASTER spectrometer at this time. While not essential for the processes discussed below, the hadronic calorimeter could well be important for other physics involving, e.g. a jet trigger. It is most likely that uranium plate (for density)-gas calorimetry will suffice. The electromagnetic part of this calorimeter may require good energy and position resolution for photons, since complete reconstruction of  $B$  decays is being proposed, but this issue has not been adequately investigated at this time.

#### H. Muon Detector

The muon detector serves both to identify muons and to provide the information for the first level muon trigger. The detector is composed of planes of trigger counters buried in steel. Both 12 and 20 GeV/c thicknesses of steel have been considered for this trigger device in Ref. 15. A configuration of trigger counters that is highly segmented and which has octant symmetry has been investigated by those authors. The trigger rates for high mass dimuon pairs ( $M > 2.5 \text{ GeV}/c^2$ ) due to pion decays, punch through, directly produced  $\psi$ 's decaying into muon pairs, and the signal ( $b \rightarrow \psi + \dots \rightarrow \mu^+ \mu^- + \dots$ ) itself have been found<sup>15</sup> to be in the range 10 to 100 per second for the 12 GeV/c thick detector. This trigger rate is close to that which might be bearable for a data acquisition and logging system at the SSC. About 5% of the total inclusive  $b \rightarrow \psi + \dots \rightarrow \mu^+ \mu^- + \dots$  rate over the entire  $4\pi$  solid angle both goes into the TASTER solid angle and survives this dimuon trigger for a 12 GeV/c thick muon detector. About 2.5% survives a 20 GeV/c thick muon detector. The relatively low momentum of the electrons from the semileptonic decays of  $B$  mesons and the muons from the  $\psi$  decay are shown in Figs. 10a and 10b, respectively. For comparison, the momentum of the muons from pion decays due to total cross section events ( $\langle n_{ch} \rangle \sim 35$  in the TASTER solid angle) is shown in Fig. 4a of Ref. 15. It is obvious from these distributions that the selection of a minimum momentum cutoff for either a single lepton or dilepton trigger is a delicate proposition. In order to preserve the signal, even at  $\sqrt{s} = 40 \text{ TeV}$ , it is essential that the cutoff not be too high; it obviously can not be too low and still achieve a finite trigger rate.

The various interferences with the accelerator by the TASTER, as represented by these eight components, have been investigated to some extent. In general, this device, which can approximately fit into one of the short ( $\pm 20$  meters), high luminosity (up to  $10^{33}/\text{cm}^2 \text{ sec}$ ) regions planned for the SSC, appears to have relatively small impact upon the machine design. Since it will not require the maximum luminosity and is relatively modest in size, it is an attractive candidate for early operation. The three areas of interference which have been considered in discussions with the Central Design Group of the SSC thus far have been: 1) the question of compensation for the relatively weak dipole field of the analysis magnet, 2) the encroachment of the muon shield on the low beta quads at the 20 meter point, and 3) the difficulty of designing a beam region vessel large enough to contain the microvertex detector described above in item A while still maintaining the machine vacuum in spite of the massive number of cable feedthroughs that would be required. These do not appear to be especially serious problems.

We consider a measurement of CP violation in the  $B$  meson system as a high sensitivity benchmark of the effectiveness of a spectrometer like the TASTER operated at the SSC. While this is the most difficult of the goals of such a detector, a demonstration of its capability for performing such a measurement would be a very significant argument for its construction. Rare  $B$  decays need a separate, extensive analysis, although it appears that a decay like  $B^+ \rightarrow K^+ \mu^+ \mu^-$  may be susceptible to a trigger strategy similar to that for measuring CP violation.

There are many general issues concerning searches of this type for CP violating asymmetries. An experiment based on the trigger  $\psi \rightarrow \ell^+ \ell^-$  (or for that matter any other characteristic of  $B$  decays that serves to separate a  $B$  signal from the total cross section) can be conducted in one of two ways. Either the trigger/tag  $B$  decay may be analyzed or the non-trigger  $B$  (which is decaying in a completely unspecified way) may be searched for after the  $b\bar{b}$  identity of the event has been established. In either case, CP violating asymmetries may appear as differences in relative decay rates for CP conjugate decays of  $B$  and  $\bar{B}$  mesons into various final states or, more sensitively, in differences of the decay time distributions of the  $B$  and  $\bar{B}$  decays. The  $B$  and  $\bar{B}$  decay modes which are being compared can result in a final state which may or may not be a CP eigenstate. CP violating asymmetries may be found in either type of decay, but the experiment must be conducted differently depending upon which type of final state is produced. If a CP eigenstate results from the decay (as is the case in many of the interesting modes involving a  $\psi$ ), then the particle or antiparticle nature of the parent  $B$  must be established by searching for and identifying the decay of the other associated  $B$  in the event. This technique is complicated if the other  $B$  is a  $B^0$  which has mixed into a  $\bar{B}^0$  (for this reason, if the other  $B$  is charged, there is less ambiguity in the determination of the parentage of the interesting decay final state) or if there is multiple  $B\bar{B}$  production in the 40 TeV event. On the other hand, if the CP violating effects are to be found by comparison of CP conjugate decays such as  $B_d^0 \rightarrow K^+ \pi^-$  versus  $\bar{B}_d^0 \rightarrow K^- \pi^+$ , the comparison can be conducted without reference to the other  $B$  decay.

In both cases, searches for CP asymmetries are complicated by potential differences in the relative initial populations of  $B$  and  $\bar{B}$  mesons. Such differences can arise from preferential

hadronization into baryons of  $b$  quarks relative to  $\bar{b}$  quarks (due to the presumably slightly larger probability of finding two light quarks in the final state of a 40 TeV  $pp$  interaction relative to the probability of finding two light antiquarks). This preferential hadronization into baryons can lead to a depletion of  $b$  quarks available for  $\bar{B}$  meson formation and, therefore, to asymmetries in the initial populations of the samples of  $B$  and  $\bar{B}$  mesons decaying into final states of interest. An experimental determination of this asymmetry (which could fake a CP violating asymmetry if not taken into account) must be undertaken. This asymmetry in initial population of  $B$  and  $\bar{B}$  mesons can be determined by the measurement of a final state such as  $B \rightarrow \psi K^- \pi^+$  and its charge conjugate which is not supposed to exhibit (according to the standard model) any CP violating asymmetries. This measurement will allow the determination of asymmetries due to experimental systematics as well as asymmetries due to different initial  $B$  and  $\bar{B}$  meson populations.

Such a technique, however, has a pitfall. The modes which are expected to show the smallest CP violating effects as predicted by the standard model may in fact be the modes which are the most sensitive to new physics. The existence of other objects (fourth generation quarks, new Higgs bosons, horizontal gauge bosons, etc) will enlarge the  $K - M$  matrix or allow for other types of CP violation which may either add to or subtract from the effects which are predicted by considering only the current players in the standard model. It may well be that the most sensitive place to look for new physics is in  $B$  decays where CP violation is expected to be small. The moral of experimentation in this area of physics may well be to "look where nothing is expected to be found" in order to have the maximum sensitivity and lever arm for detecting new effects.

All of the above considerations must be taken into account in evaluating the capabilities of the TASTER for detecting CP violating effects. An investigation of the sensitivity for doing CP searches has been carried out in Ref. 15 using the strategy of triggering and tagging on the  $b \rightarrow \psi + \dots \rightarrow \mu^+ \mu^- + \dots$  decays. The authors of this paper find, using Monte Carlo calculations of the TASTER acceptance and estimates of various experimental efficiencies, that 3900  $B_d$  or  $\bar{B}_d \rightarrow \psi \phi \rightarrow \mu^+ \mu^- K^+ K^-$  decays (with the opposite side  $B_u$  identified as to its charge) can be accumulated in a one year run ( $10^7$  seconds) at a luminosity of  $10^{32}/\text{cm}^2 \text{ sec}$  if the branching ratios given in Ref. 31 are correct, and if strategies can be developed whereby as much as 5% of the opposite side  $B_u^\pm$  can be determined to be a  $B$  or  $\bar{B}$ . A 2% difference due to CP violation is expected<sup>31</sup> between the partial rates for  $B$  and for  $\bar{B}$  decaying into this final state (about a one sigma effect).

The same sort of evaluation, but searching for CP violating asymmetries in the decays  $B_d$  or  $\bar{B}_d \rightarrow \psi K_S$  yields a sample of 2600 events (with an opposite side  $B_u$  identified as to its charge) within which to detect an estimated 8% asymmetry (about a 3 sigma effect). The comparison of these two examples serves to point out the advantages which larger asymmetries produce. Since the statistical error decreases as  $1/\sqrt{N}$ , the smaller asymmetries are more difficult to see even if there is a larger data sample available for the search. These sorts of studies, as done thus far, have only roughly estimated some of the factors necessary for determining the size of the final data sample that can be accumulated in a few modes. Many other modes, where the asymmetries and branching rates may

be larger or smaller need to be investigated. Furthermore, if strategies for more effective tagging (assumed to be 5% of the  $B_u$ 's in these analyses) of the particle or antiparticle nature of the decaying meson can be developed, as through semileptonic decays, then the statistical significance of the measurements under discussion can be greatly improved. In addition, searches for differences in the time distributions between certain  $B$  and  $\bar{B}$  modes (like  $B_s \rightarrow D^- K^+$  versus  $\bar{B}_s \rightarrow D^+ K^-$ ) may be a much more sensitive way of searching for CP asymmetries. Finally, the summing of various exclusive modes may be attempted to increase statistics. As things now stand, much remains to be done, but the development of a trigger strategy is quite encouraging. While difficult, detection of CP violation in the  $B$  system seems at least within the realm of feasibility at the SSC with a tailored device such as the TASTER.

### References

1. See, for example, the summary reports of I. Hinchliffe, of J. W. Cronin et al., and of K. Lane, in *Proceedings of the 1984 Summer Study on the Design and Utilization of the SSC*, edited by R. Donaldson and J. G. Morfin (American Physical Society, New York, 1984), p. 1, p. 161, and p. 729 and references therein. We refer to these proceedings as SNOWMASS 84.
2. See R. J. Morrison, in *Proceedings of the Seventh Vanderbilt Conference on High Energy Physics*, Nashville, May 15-17, 1986 (to be published), and M. Losty, in *Proceedings of the 1986 SLAC Summer Institute on Particle Physics*, July 28 - August 8, 1986 (to be published).
3. J. C. Collins, D. E. Soper and G. Sterman, *Nucl. Phys. B263*, 37 (1986).
4. R. K. Ellis, in *Proceedings of the XXI Rencontre de Moriond: Strong Interactions and Gauge Theories*, Les Arcs, France, March, 1986 (to be published), and Fermilab preprint FERMILAB-CONF-86/35-T, 1986 (unpublished).
5. D. W. McKay and J. P. Ralston, these Proceedings.
6. D. B. Cline, in *Proceedings of the Madison Workshop on Physics Simulations at High Energies*, May, 1986 (to be published).
7. E. L. Berger, J. C. Collins and D. E. Soper, these Proceedings.
8. A. Kernan and D. Smith, presentations to the Heavy Flavor Working Group sessions.
9. P. F. Shepard, these Proceedings.
10. F. E. Paige and S. D. Protopopescu, "ISAJET 5.90: A Monte Carlo Event Generator for  $pp$  and  $p\bar{p}$  Interactions", these Proceedings.
11. T. D. Gottschalk, in *Proceedings of the UCLA Workshop on Observable Standard Model Physics at the SSC: Monte Carlo Simulation and Detector Capabilities*, edited by H.-U. Bengtsson, C. Buchanan, T. Gottschalk, and A. Soni (World Scientific, Singapore, 1986), p. 122.
12. A. H. Mueller and J. Nason, *Phys. Lett.* **157B**, 226 (1985).
13. M. G. D. Gilchriese, SNOWMASS 84, p. 523 and references therein.
14. G. Hanson and D. Meyer, SNOWMASS 84, p. 585 and references therein.
15. B. Cox and D. E. Wagoner, these Proceedings.
16. R. S. Panvini and T. Reeves, these Proceedings.
17. K. Lane and J. Rohlf, SNOWMASS 84, p. 737.
18. E. W. N. Glover and T. D. Gottschalk, these Proceedings.
19. T. D. Gottschalk, these Proceedings.
20. G. Arnison *et al.*, *Phys. Lett.* **122B**, 103 (1983).
21. B. Cox and F. J. Gilman, SNOWMASS 84, p. 87.
22. F. J. Gilman and L. E. Price, these Proceedings.
23. H.-U. Bengtsson and T. Sjostrand, University of Lund preprint, 1986 (unpublished).
24. D. Hedin, presentations to the Heavy Flavor Working Group sessions and private communication.
25. J. F. Gunion and A. Savoy-Navarro, in *Proceedings of the 1986 UCLA Workshop on Observable Standard Model Physics at the SSC: Monte Carlo Simulation and Detector Capabilities*, edited by H.-U. Bengtsson, C. Buchanan, T. Gottschalk, and A. Soni (World Scientific, Singapore, 1986), p. 338.
26. S. Kim, these Proceedings.
27. G. Kane, F. Paige, L. Price and M. Goodman, in *Proceedings of the Workshop on Triggering, Data Acquisition, and Computing for High Energy/ High Luminosity Hadron - Hadron Colliders*, edited by B. Cox, R. Fenner, and P. Hale (Fermilab, Batavia, 1986), p. 1.
28. E. W. N. Glover and D. A. Morris, these Proceedings.
29. N. G. Deshpande and A. Soni, these Proceedings and references therein.
30. L. L. Chau, these Proceedings and references therein.
31. I. Dunietz, presentation to the Heavy Flavor Working Group sessions and I. Dunietz and J. L. Rosner, *Phys. Rev. D* **34**, 1404 (1986) and D.-S. Du, I. Dunietz, and D.-D. Wu, Institute for Advanced Study preprint, 1986 (unpublished).
32. I. I. Bigi, SLAC preprint SLAC-PUB-4074, 1986 (unpublished) and references therein.
33. J. A. Appel *et al.*, in *Proceedings of the Workshop on Triggering, Data Acquisition, and Computing for High Energy/ High Luminosity Hadron - Hadron Colliders*, edited by B. Cox, R. Fenner, and P. Hale (Fermilab, Batavia, 1986), p. 269.
34. J. Butler, these Proceedings.
35. T. Kondo, M. Nakamura, K. Niwa, and Y. Tomita, SNOWMASS 84, p. 612.
36. C. D. Buchanan and Y. Oyang, these Proceedings.